EFFECT OF TRAINING OVERHEAD ON THE PERFORMANCE OF MILLIMETER WAVE CHANNEL ESTIMATION MODELS

Akeem Abimbola RAJI[1], Isaiah Adediji ADEJUMOBI[2], Joseph Folorunso ORIMOLADE[3], Kamoli Akinwale AMUSA[4], Olakunle Elijah OLABODE[5]
[1,5]Department of Electrical and Electronics Engineering, Faculty of Engineering, Olabisi Onabanjo University, Ago-Iwoye, Ogun State, Nigeria
[2,4]Department of Electrical and Electronics Engineering, College of Engineering, Federal University of Agriculture, Abeokuta, Nigeria
[3]Department of Electrical and Electronics Engineering, College of Engineering, Afe-Babalola University, Ado-Ekiti, Nigeria.
[1]rajiakeemabimbola@gmail.com, [2]adejumobiia@funaab.edu.ng, [3]orimoladejf@abuad.edu.ng, [4]amusaka@funaab.edu.ng, [5]olabode.olakunle@oouagoiwoye.edu.ng

Keywords: estimation models, fifth generation, millimeter wave channel, quantization, training overhead

Abstract: *The increasing demand for enormous data rate is propelling interest in 5G millimeter wave communication. Several methods have been proposed for millimeter wave channel estimation but there is little or dearth of information on the impact of training overhead on the performance of these methods. This work investigated the effect of training overhead on the performance of orthogonal matching pursuit (OMP), compressed sampling matching pursuit (CoSAMP), deep learning (DL) and least square (LS) techniques by employing normalized mean square error (NMSE), spectral efficiency (SE) and bit rate as performance indices. It was observed from NMSE profile that smallest errors were recorded for DL and OMP when the training overhead was 60 while for COSAMP and LS, lowest errors were recorded when the training overheads were 55 and 65, respectively for 4-bit ADC. It was seen also that, SE and bit rate exhibited dissimilar characteristics over increasing values of training overheads.*

1. INTRODUCTION

Increasing mobile subscriber density occasioned by improved access to the internet, has necessitated the need for expanding communication bandwidth. As a result, millimeter wave frequency band is being considered as a new paradigm for communication not only for improving user experience on the internet but also for coping with the rapid growth of mobile subscriber density, avoiding network congestion, and for meeting increasing mobile data rate demand. Fifth Generation (5G) network access has been deployed using millimeter wave band for improving latency, increasing throughput and enhancing spectral access. Other importance of millimeter wave network access is well documented in the literature [1-7]. Several works have designed millimeter wave architecture for accomplishing enormous gains of the millimeter wave band where the importance is stressed of a good deal of knowledge of the propagation environment. Consequently, literature has been agog with different methods for carrying out the task of estimating millimeter wave channel.

The techniques proposed include adaptive compressed sensing [8], orthogonal matching pursuit [9-12], least square technique [11], estimation of signal parameters via rotational invariance [13], deep learning technique [14-15], low tensor technique [16], multiple signal classification [17], subspace technique [18] and compressed sampling matching pursuit [19]. Authors in [20] propose expectation maximization and generalized approximate passing. As remarkable as findings in the existing works are, there is little or dearth of information on the impact of training overhead on the performance of millimeter wave channel estimation methods. This work investigates the effect of training overhead on the performance of least square technique (LS), orthogonal matching pursuit (OMP), compressed sampling matching pursuit (CoSAMP) and deep learning (DL)

techniques which are used here as candidates for investigation. The paper is structured as follows: section one is the introduction, section 2 presents problem formulation and approaches adopted for solving the problem, section 3 is the results and discussion and section 4 gives concluding remarks.

2. MATERIALS AND METHODS

2.1 Modelling of millimeter wave cellular system

Figure 1 depicts millimeter wave cellular system consisting of a transmitting station (TS) for combining multiple N_s streams which are transmitted via N_{TS} antenna to the Receiving station (RS) where the transmitted packets are received by N_{RS} antennas. The received streams are down- converted to the carrier frequency, quantized by analog to digital converter (ADC) and digitally combined at RS using digital combiner. The received signal at RS is expressible in a form given by [21] as:

$$y = M_{BB}^{H}\mathbb{Q}\left(M_{Rf}^{H}HN_{RF}N_{BB}u + M_{Rf}^{H}g\right) \quad (1)$$

wherein $y \in N_s \times 1$is the received spatial stream, $N \in N_{BB}N_{RF}$ is the precoder at TS, for which $N_{RF} \in \mathbb{C}^{N_{TS}\times P_{TS}^{RF}}$ is the analog precoder matrix and $N_{BB} \in \mathbb{C}^{P_{TS}^{RF}\times N_s}$is the digital precoder matrix, $M \in M_{RF}M_{BB}$ is the combiner at RS, for which $M_{RF} \in \mathbb{C}^{N_{RS}\times P_{RS}^{RF}}$ is the analog combiner matrix, $M_{BB} \in \mathbb{C}^{P_{RS}^{RF}\times N_s}$ is the digital combiner matrix while $(.)^H$is the symbol for conjugate transpose.

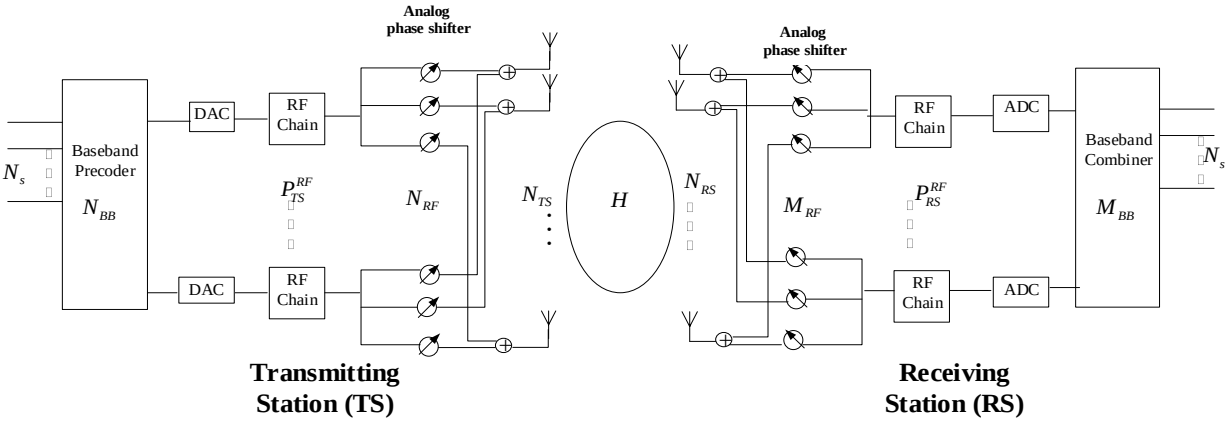

Fig. 1 Millimeter wave cellular system model [21]

$\mathbb{Q}(.)$ denotes quantization operator, u is the transmitted spatial symbol, $g$symbolizes the noise vector while H represents millimeter wave propagation channel which is modelled using equation (2) as given by [10], [19], and [20] as:

$$H = \sqrt{\frac{N_{TS}N_{RS}}{L}}\sum_{t=1}^{L}\sigma_t p_{Rs}(\theta_t)p_{TS}^{H}(\varphi_t) \quad (2)$$

in which, the number of paths between TS and RS is represented by$L$, $\sigma_t$is the complex channel gain, independent and identically distributed, $p_{Rs}(\theta_t)$ symbolizes array steering vector with θ_t representing azimuth angle of arrival at RS and $p_{Ts}(\varphi_t)$is the array steering vector for which φ_t is the azimuth angle of departure from TS. It is assumed that the millimeter wave cellular system utilizes uniform linear array for radiation at TS and the same is also used for reception at RS and in that connection, array steering vectors at TS and RS are written as:

$$p_{TS}(\varphi_t) = \sqrt{\frac{1}{N_{TS}}}\begin{bmatrix}1, e^{j\frac{2\pi}{\lambda}z\sin(\varphi_t)}, e^{j\frac{4\pi}{\lambda}z\sin(\varphi_t)}, \dots,\\ e^{j(N_{TS}-1)\frac{2\pi}{\lambda}z\sin(\varphi_t)}\end{bmatrix}^T \quad (3)$$

$$p_{RS}(\theta_t) = \sqrt{\frac{1}{N_{RS}}}\begin{bmatrix}1, e^{j\frac{2\pi}{\lambda}z\sin(\theta_t)}, e^{j\frac{4\pi}{\lambda}z\sin(\theta_t)}, \dots,\\ e^{j(N_{RS}-1)\frac{2\pi}{\lambda}z\sin(\theta_t)}\end{bmatrix}^T \quad (4)$$

where $z = \frac{\lambda}{2}$ is the spacing between the array elements and λ is the operating wavelength.

According to Hassan et al. [22], equation (2) may be represented by virtual form as:

$$H = P_{RS}(\alpha)P_{TS}^{H} \quad (5)$$

in which α is a matrix containing the path gain σ_t P_{TS} and P_{RS}, are array response matrices which admit expressions of the forms of equations (6) and (7) as:

$$P_{TS} = [p_{TS}(\varphi_1), p_{TS}(\varphi_2), \dots, p_{TS}(\varphi_L)] \in \mathbb{C}^{N_{TS}\times L} \quad (6)$$

$$P_{RS} = [p_{RS}(\theta_1), p_{RS}(\theta_2), \dots, p_{RS}(\theta_L)] \in \mathbb{C}^{N_{RS}\times L} \quad (7)$$

Based on the millimeter channel model of equation (5), estimated millimeter wave channel admits expression of the form:

$$\bar{H}^{e} = \bar{P}_{RS}(\mu)\bar{P}_{TS}^{H} \quad (8)$$

where $\bar{H}^{e}$ is the estimated millimeter wave channel whose entries are expected to be close to the entries of channel model of equation (5), $\bar{P}_{RS}$ and $\bar{P}_{TS}$ are estimated array matrices whose angles of arrival and departure are divided into F_{TS} and F_{RS} grid sizes and μ is the sparse matrix consisting of channel gain.

In estimating components of equation (8), it is assumed that TS transmits identical symbol using training precoder during S training instants and RS utilizes training combiner with the received signal at RS being expressed by

$$y = \mathbb{Q}\left(\sqrt{\beta}(A_s^{H}\bar{H}^{e}B_s + A_s^{H}g_s)\right) \quad (9)$$

wherein β denotes average received power, A_s and B_s are training combiner and precoder, respectively and $s = 1,2,3 \dots, S$ is the amount of training overheads over which the channel estimation is carried out. By representing equation (9) in vector form leads to equation (10) expressed by:

$$w = \mathbb{Q}\left(\left(\sqrt{\beta}\left(B_s^{T} \otimes {A_s}^{H}\right)vec[\bar{H}^{e}] + d\right)\right) \quad (10)$$

w is the resulting received signal and $d = diag\left[{A_s}^{H}vec(g_s)\right]$ is the additive white Gaussian noise vector. In equation (10), vector identity $vec(XYZ) = Z^{T} \otimes Xvec(Y)$ is invoked, where, $\otimes$ is the symbol for Kronecker product of two vectors.

When equation (8) is substituted in equation (10), the following equation suffices;

$$w = \mathbb{Q}\left(\left(\sqrt{\beta}\left({B_s}^{T} \otimes {A_s}^{H}\right)(\bar{P}_{TS}^{*} \otimes \bar{P}_{RS})vec(\mu) + d\right)\right) \quad (11)$$

It is of interest to note that B_s and A_s are parameters which are constructed with entries deduced from random values of equation (12) and (13) given by [10], [19] and [21] as:

$$[B]_{i,k} = \frac{1}{\sqrt{N_{TS}}}e^{j\frac{a_Q 2\pi}{2^{N_q^{TS}}}} \quad (12)$$

$$[A]_{i,k} = \frac{1}{\sqrt{N_{RS}}}e^{j\frac{a_R 2\pi}{2^{N_q^{RS}}}} \quad (13)$$

For which N_q^{TS}, N_q^{RS} respectively, are the amount of quantization bits in the analog phase shifter at TS and RS.

By invoking that $\Phi = \left({B_s}^{T}\bar{P}_{TS}^{*} \otimes \bar{P}_{RS}{A_s}^{H}\right)$ and $a = vec(\mu)$ in equation (11) leads to underdetermined linear problem expressed by equation (14) as:

$$w = \mathbb{Q}\left(\sqrt{\beta}\Phi a + d\right) \quad (14)$$

where Φ is the sensing matrix and a represents unknown sparse channel gain. All other parameters remain as defined earlier.

The quantization operator in equation (14) is modelled as uniform mid-rise quantizer with quantization step given by [21] as:

$$\Delta = \frac{q}{2^{v-1}} \quad (15)$$

For which, Δ denotes quantization step, v represents quantity of bits in the ADC and q denotes maximum absolute value of real and imaginary parts of measurement vector, w. Equation (14) is solved for the channel gain using quantized versions of OMP, CoSAMP, and DL models available in the literature [21] which are described as follows.

2.2. Channel estimation methods

2.2.1. OMP model

The following algorithm steps are implemented in determining the channel gain via OMP

Step 1: largest inner product between sensing matrix and the residual is determined for which the residual is equal to measurement vector for the first instance. This forms the current support entries.
Step 2: enlarged support is formed by finding the union between the current support and previous support estimate.
Step 3: least square problem over the enlarged support is determined for the channel gain.
Step 4: The residual is updated
Step 5: The process is repeated until the norm of the residual is less than a given threshold
Step 6: End the process

2.2.2 CoSAMP model

The algorithm steps of CoSAMP model are as follows:

Step 1: correlation between the sensing matrix and residual is computed.

Step 2: The largest components of the correlation are identified which form the new supports

Step 3: new supports are combined with the sets from the previous estimates.

Step 4: Channel gain emerges by solving least square problem over the current or enlarged support.

Step 5: gain is pruned down such that its length is equal to the sparsity of the millimeter wave channel.

Step 6: residual is updated

Step 7: repeat the process until the norm of the residual is less than the defined threshold

Step 8: End the process

2.2.3. Deep learning model

A dense multilayer perceptron feed forward neural network (a variant of deep learning) is modelled for determining the channel gain where the network consists of input layer, three hidden layers and output layer [21]. Given an input vector,x_n of *n*-th elements, the output of the deep learning neural network, y_o, is expressed by:

$$y_o = \varphi_o\left(\sum_{j=1}^{M} w_{1j}\left(\varphi_h(\sum_{n=1}^{N} w_{in}x_n)\right)\right) \quad (16)$$

in which φ_o, φ_h, respectively represent activation functions at the output and hidden layers, $w_{1j}$is the connection weight between neuron j in the hidden layer and output layer, w_{in} is the synaptic weight between neurons at the hidden layer and input layer. x_n is obtained from correlation of sensing matrix and measurement vector. The weights of the network are trained by using back propagation algorithm, where the error expressed by (17) is propagated to the hidden layers for proper training of the weights.

$$k = f - y_o \quad (17)$$

where $k$denotes the propagation error and $f$is the expected output (gain of the simulated millimeter wave channel environment).

2.2.4. Least Square (LS) model

The least square channel estimate is determined from equation (10) by minimizing error function given by;

$$f(\bar{H}^{LS}) = \sqrt{\beta}(\|w - G\bar{H}^{LS}\|_2^2) \quad (18)$$

where, $f(\bar{H}^{LS})$ is the error function to be minimized, $\bar{H}^{LS}$ is the least square channel estimate and $G = B_s^T \otimes {A_s}^H$. Equation (18) is expanded further as:

$$f(\bar{H}^{LS}) = \sqrt{\beta}\left((w - G\bar{H}^{LS})^H(w - G\bar{H}^{LS})\right) \quad (19)$$

By invoking symmetry and equating the derivative of equation (19) to zero, $\bar{H}^{LS}$ is expressible as:

$$\bar{H}^{LS} = \frac{1}{\sqrt{\beta}}(G^H G)^{-1} G^H w \quad (20)$$

2.3. Performance metrics

The performance of channel estimation models is evaluated by using normalized mean square error (NMSE), spectral efficiency and bit rate as metrics and are defined as:

$$NMSE(dB) = 10\, log_{10}\left[\frac{\|H - \bar{H}^e\|_F^2}{\|H\|_F^2}\right] \quad (21)$$

where $\| \ \|_F$ is the symbol that represents the Frobenius norm between two matrices

Spectral efficiency

$$= log_2\left|I_{N_s} + \frac{SNR}{N_s}(M^H M)^{-1} M^H H N N^H H^H M\right| \quad (22)$$

where $N$is the left-hand singular matrix from the singular value decomposition of channel estimate $\bar{H}^e$ or $\bar{H}^{LS}$ while M is a combiner designed using the approach presented in [24].

Bit rate = spectral efficiency × bandwidth (23)

3. RESULTS AND DISCUSSION

Here, simulation results that illustrate the impact of training overheads on the performance of millimeter wave channel estimation models are presented.

The results are generated using simulation code written in R2018a Matlab environment and whose implementation is done on Intel(R) Core (TM) i3-5005U@ 2.00GHz.

A single user millimeter wave cellular system consisting of N_{TS}= 64 antennas at TS and N_{RS}= 32 antennas at RS is assumed with 7 channel paths between TS and RS. The amount of RF chains at both TS and RS is 5, bandwidth is 500MHz while operating frequency is 32GHz [19]. The entries of the millimeter wave channel model H in equation (2) are constructed by assuming that its angles of departure and angle of arrival are distributed over $(0,2\pi)$ and gain assumed to be independent and identically distributed [19] and [21].

For the purpose of determining corresponding channel estimates, $\bar{P}_{TS}$ and $\bar{P}_{RS}$ matrices in equation (8) consist of entries whose angles of departure and angle of arrival are uniformly distributed on discretized grids $F_{TS} = N_{TS}$ and $F_{RS} = N_{RS}$. Complex Gaussian random values are used to model AWGN, taken from $\mathbb{CN}(0, \tau^2)$where τindicates the noise power. The power received, symbolized, by $\beta = \tau^2 \times SNR$ with SNR denotes signal to noise ratio in decibel. CoSAMP and OMP algorithms are stopped when the norm of the residual falls below 10^{-10} [19]. The DL neural network model consists of 512, 256 and 128 dense neurons, respectively in each of the three hidden layers and the network allows for 20% dropout of hidden neurons. The quantity of epochs for training the weight is 1200 and learning rate is 0.01 [21].

Figure 2 presents the response behavior of NMSE to change of SNR from -20dB to 20dB where S varies from 50 to 70 and the quantity of bits in the ADC (v) is 4.

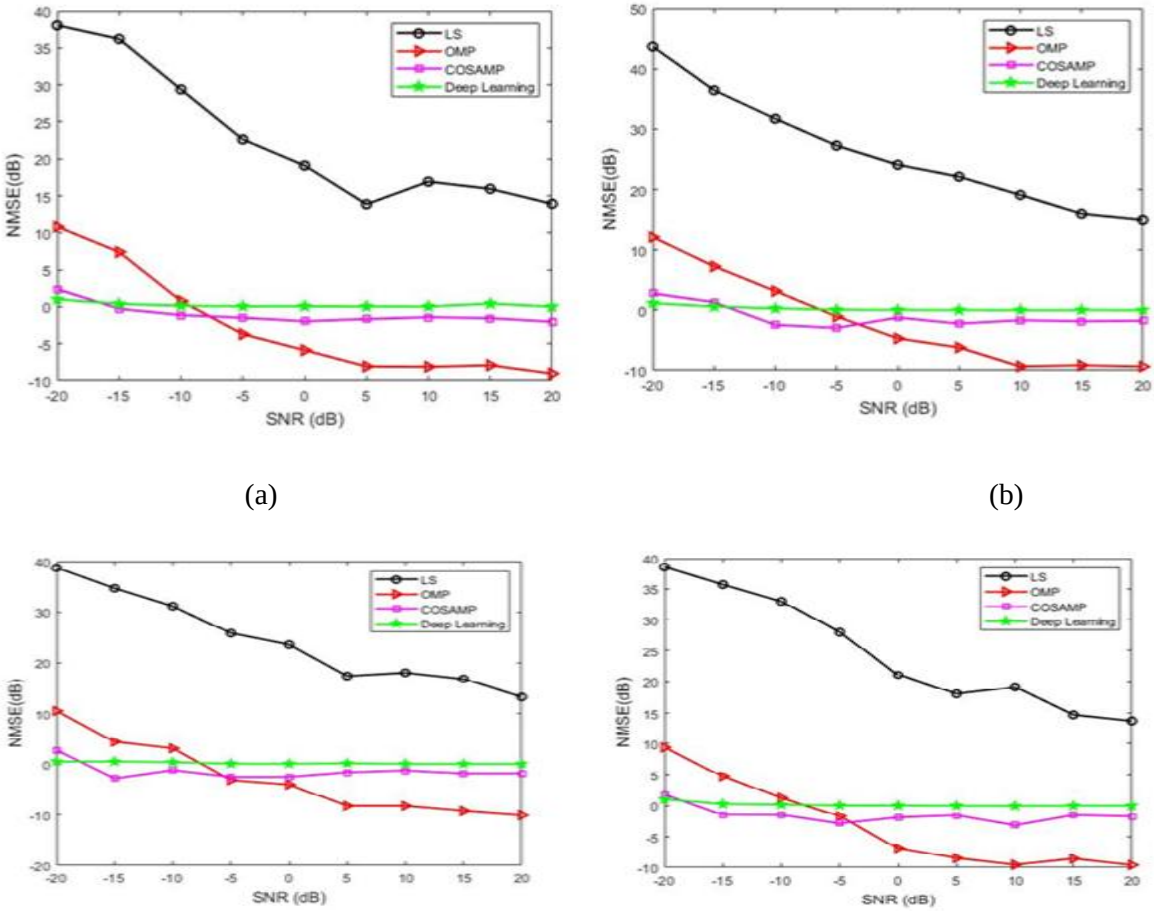

Fig. 2. NMSE characteristics of OMP, CoSAMP, LS and DL, $v = 4$ and S is (a) 50, (b) 55, (c) 60 and (d) 70

It is observed in Fig. 2 that LS displays the worst performance as SNR increases from -20dB to 20dB and for all the values of training overhead. It is observed also in Fig. 2 that OMP exhibits the best performance when SNR is beyond -10dB as shown in Figs. 2(a), -5dB as observed in Fig. 2(b) and 5dB as seen in Figs. 2(c) and 2(d).

Figure 3 on the other hand depicts computational profiles where NMSE is varied against number of training overhead, S, and using SNR of 15dB and 4 bit ADC.

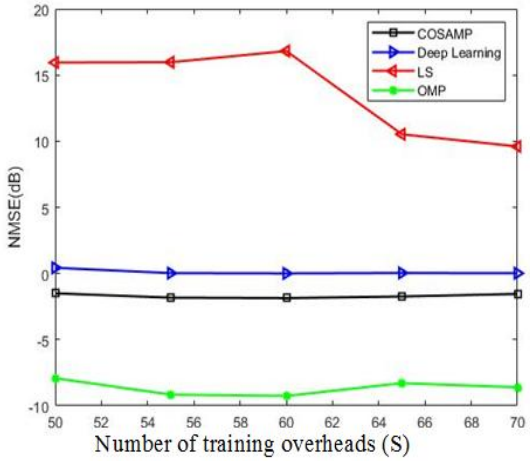

Fig 3. NMSE against number of training overheads, $v = 4$ and SNR = 15dB

A closer look at Fig. 3 shows that NMSEs of OMP and DL slightly reduce with increase in

training overhead from 50 to sixty 60 beyond which the errors marginally increase. The values of NMSE for OMP at training overheads of 50, 55, 60, 65 and 70 are -7.9, -9, -9.3, -8.3 and -7.9dB, respectively while NMSEs for DL are 0.4, 0.03, 0.007, 0.039 and 0.021dB, respectively. It is noticed that both OMP and DL have the lowest errors when the training overhead is 60.

Moreover, it is seen in Fig. 3 that NMSE of COSAMP surges when the training overhead is beyond 55. The values of NMSE for CoSAMP at training overhead of 50, 55, 60, 65, and 70 are -1.5, -2, -1.86, -1.7, and -1.5dB, respectively. This indicates that CoSAMP has lowest error at training overhead of 55. Figure 3 also shows that there is an initial rise of NMSE of LS from training overhead of 50 to 60 after which NMSE reduces significantly. The values of NMSE for LS at training overheads of 50, 55, 60, 65, and 70 are 15.9, 16, 17, 10.5 and 9.5dB, respectively. It is found that LS has the smallest error when the training overhead is 65. This suggests that LS requires more training overhead and greater higher computational resources than others.

In addition, Figs. 4 and 5 illustrate spectral efficiency and bit rate against SNR where $v = 4$ and S is varied from 50 to 70.

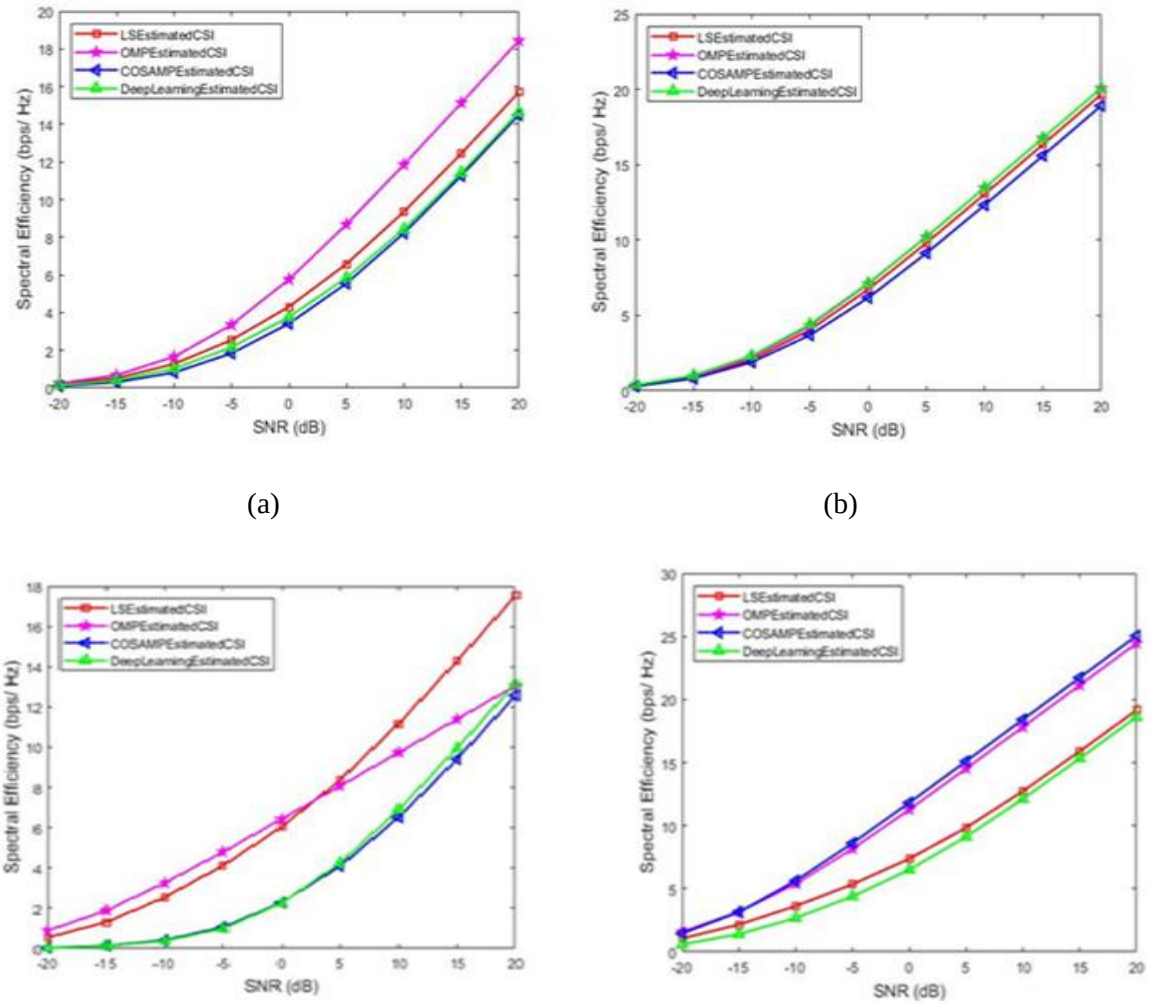

Fig.4 Spectral efficiency characteristics of OMP, CoSAMP, LS and DL, $v = 4$ and S is (a) 50, (b) 55, (c) 60 and (d) 70

Figure 4 reveals that the spectral efficiencies of all the channel estimation models increase linearly across SNR for all the values of training overhead utilized as candidates for investigation. Computational profiles for bit rate in Fig. 5 also exhibit similar characteristics to that of spectral efficiency. Furthermore, it is observed in Figs. 4 (a) and 5 (a) that OMP has the best spectral efficiency and bit rate when S is 50 and across all the values of SNR while in Figs. 4(b) and 5(b), DL has the greatest spectral efficiency and bit rate when S is 55.

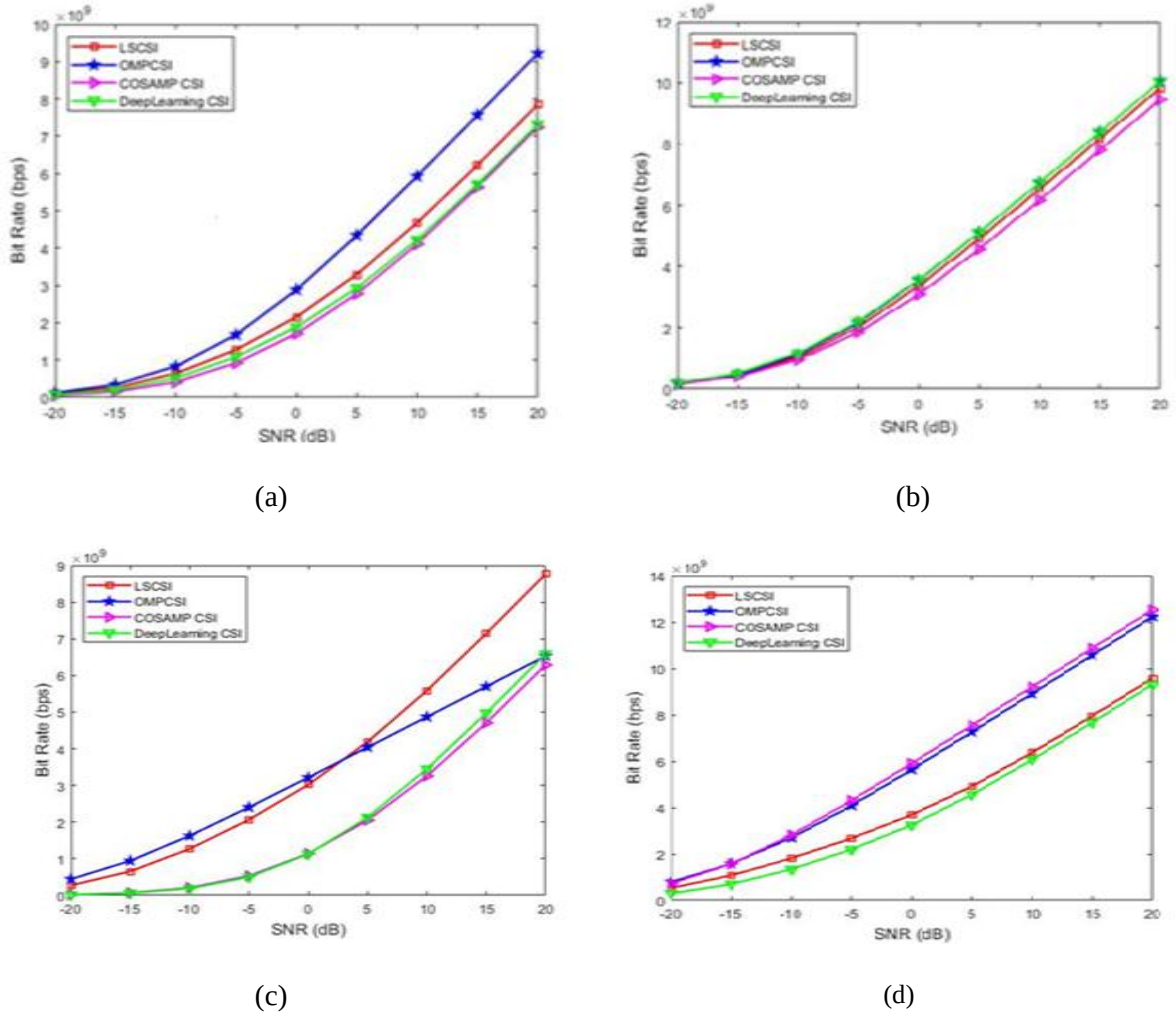

Fig. 5 Bit rate characteristics of OMP, CoSAMP, LS and DL, $v = 4$ and S is (a) 50, (b) 55, (c) 60 and (d) 70

It is however seen in Figs. 4(c) and 5(c) that OMP exhibits the best performance when S is 60 and when SNR is between -20dB and 4dB, beyond which LS outperforms OMP and has the best spectral efficiency and bit rate over the range of 4dB to 20dB.

In addition, when training overhead is increased to 70 and as shown in Figs. 4 (d) and 5 (d), CoSAMP has the best spectral efficiency and bit rate.

4. CONCLUSION

This work investigated the effect of training overhead on the performance of four-millimeter wave channel estimation models which included orthogonal matching pursuit, least square, compressed sampling matching pursuit and deep learning. Normalized mean square error (NMSE), spectral efficiency and bit rate were utilized as candidates for evaluating the performance of those channel estimation models. It was seen for

all the values of training overheads that NMSE of LS displayed the worst performance over SNR values considered. In addition, it was observed from NMSE profiles using 4-bit Analog to Digital Converter (ADC) that OMP and DL recorded the lowest errors when the training overhead was 60 while lowest error was observed for CoSAMP when the training overhead was 55. Furthermore, it was found that LS required 65 as training overhead which implied that more training overheads were needed for reduced error performance in LS. This suggested that LS would require more computational resources than other models.

In addition, it was found that spectral efficiency and bit rate of all the estimation models increased linearly with increasing values of SNR and training overhead. It was seen that spectral efficiency and bit rate of these models exhibit varying characteristics under different values of training overhead with OMP producing the best spectral efficiency and bit rate when the training overhead was 50 while DL has the highest spectral efficiency and bit rate when training overhead was increased to 55. Compressed sampling matching pursuit produced the best performance on increasing the training overhead to 70. This study indicated that the training overhead played pivotal role in the behavior of normalized mean square error, spectral efficiency and bit rate of these models.

The impact of training overhead on the performance of other millimeter wave channel estimation methods existing in the literature will be considered in future.

5. REFERENCES

[1] Raji, A.A., Adejumobi, I.A., Orimolade, J.F., Amusa, K.A., and Olajuwon, B.I. *"Requirements and potentials of millimeter wave cellular systems"*, International Journal of Basic Science and Technology, vol. 8, no. 3, pp. 284-290, 2022

[2] Wei, L., Hu, R.Q., Qian, Y. and Wu, G. "*Key elements to enable Millimeter wave communication for 5G wireless systems",* IEEE wireless communications, pp. 136-143, 2014.

[3] Xiao, M., Mumtaz, S., Huang, Y., Dai, L., Li, Y., Matthaiou, M., Karagiannidis, G.K., Bjornson, E., Yang, K., Chin-Chin, I. and Ghosh, A, *"Millimeter wave communications for future mobile networks",* IEEE Journal of Selected Areas in Communications, vol. 35, no.9, pp. 1909-1935, 2017.

[4] Mohapatra, S.K., Swain, B.R., Pati, N. And Pradhan, A. *"Road towards Millimeter wave communications for 5G Network: a technological overview",* Transactions on machine learning and Artificial Intelligence, vol. 2, issue 5, pp. 48-60, 2014.

[5] Rappaport, T.S., MacCartney, G.R., Samimi, M.K. and Sun, S. *"Wideband millimeter-wave propagation measurements and channel models for future wireless communication system design",* IEEE Transactions on Communications, vol. 63, no. 9, pp. 3029-3056, 2015.

[6] Akdeniz, M.R., Liu, Y., Samimi, M.K., Sun, S., Rangan, S., Rappaport, T.S. and Erkip, E. *"Millimeter wave channel modelling and cellular capacity evaluation",* IEEE Journal of Selected Areas in Communication, vol. 32, no. 6, pp. 1164-1179, 2014.

[7] Heath, R.W., Nuria, G.P., Rangan, S. and Akbar, S. *"An overview of signal processing techniques for millimeter wave MIMO systems",* IEEE Journal of Selected Topics in Signal Processing, vol. 10, no. 3, pp. 436-453, 2016.

[8] Alkhateeb, A., Ayach, O.E., Leus, G. and Heath, R.W. *"Channel estimation and hybrid precoding for Millimeter-wave cellular systems",* IEEE Journal of Selected Topics in Signal Processing, vol. 8, no. 5, pp. 831-846, 2014

[9] Alkhateeb, A., Leus, G. and Heath, R-W *"Compressed sensing based multi-user Millimeter wave systems: How Many measurements are needed?",* In Proceedings of 2015 IEEE International Conference on Acoustics, Speech and Signal Processing, Brisbane, QLD, Australlia, 19-24 April, 2015.

[10] Venugopal, K., Alkhateeb, A., Gonzalez-Preclic, N. and Heath, R-W *"Channel estimation for hybrid architecture based wideband millimeter wave systems"*, IEEE Journal on selected areas in communications, vol. 35, no. (9), pp. 1996-2009, 2017.

[11] Lee, J., Gil, G.T. and Lee, Y.H. *"Channel estimation via orthogonal matching pursuit for hybrid MIMO systems in millimeter wave communications",* IEEE transactions on communications, vol. 64, no. 6, pp. 2370-2386, 2016.

[12] Mendez Rial, R., Rusu, C., Gonzalez-Preclic, N., Alkhateeb, A. and Heath, R.W. "*Hybrid MIMO architectures for millimeter wave communications: phase shifters or switches",* IEEE Access, vol. 4, pp. 247-267, 2015.

[13] Liao, A., Gao, Z., Wu, Y., Wang, H. and Alouini, M.S "*2D unitary ESPIRIT based super-resolution*

channel estimation for millimeter wave massive MIMO with hybrid precoding", IEEE Access, vol. 5, pp. 24747-24757, 2017.

[14] Ma, W., Qi, C., Zhang, Z., and Cheng, J, *"Deep learning for compressed sensing based channel estimation in millimeter wave massive MIMO",* In Proceedings of 2019 11th International Conference on Wireless Communications and Signal Processing (WCSP), 2019.

[15] Raji, A.A., Adejumobi, I.A., Orimolade, J.F., Amusa, K.A., and Olajuwon, B.I. *"Channel estimation for Millimeter wave MIMO systems via deep learning"*, International Journal of Basic Science and Technology, vol. 8, no. 3, pp. 276-283, 2022.

[16] Zhou, Z., Fang, J., Yang, L., Li, H., Chen, Z. and Blum, R.S *"Low-rank tensor decomposition-aided channel estimation for Millimeter wave MIMO-OFDM system"*, IEEE Journal of Selected Areas on Communication, vol. 35, no. 7, pp. 1524-1538, 2017.

[17] Guo, Z., Wang, X., and Heng, W, *"Millimeter-wave channel estimation based on 2D-beamspace MUSIC method",* IEEE Transactions on Wireless Communications, vol. 16, no. 8, pp. 5384-5394, 2017.

[18] Ghauch, H., Kim, T., Bengtsson, M. and Skoglund, M. "*Subspace estimation and decomposition for large Millimeter wave MIMO systems"*, IEEE Journal of Selected Topics in Signal Processing, vol. 10, no. 3, pp. 528-542, 2016.

[19] Raji, A.A., Orimolade J.F., Adejumobi I.A., Amusa K.A., and Olajuwon B.I. "*Channel Estimation via Compressed Sampling Matching Pursuit for Hybrid MIMO Architectures in Millimeter Wave Communication*", International Journal of Electronics Letters,2024,https:doi.org/10.1080/21681724.2024.2410061

[20] Mo, J., Schniter, P., Prelcic, N-G. and Heath, R.W. *"Channel estimation in millimeter wave MIMO Systems with one-bit quantization",* In Proceedings of 2014 48th IEEE Asilomar Conference on Signals, Systems and Computers, pp. 2-5, 2014.

[21] Raji, A.A., Orimolade, J.F., Amusa, K.A., and Adejumobi, I.A. "*Channel estimation and MIMO combining architecture in Millimeter wave cellular system with few ADC bits",* Journal of Engineering and Applied Science, vol. 70, no. 40, pp. 1-20.

[22] Hassan, K., Masarra, M., Zwingelstein, M., and Dayoub, I. "*Channel estimation techniques for millimeter-wave communication systems: Achievements and Challenges*", IEEE Open Journal of the Communications Society, vol. 1, pp. 1336-1363, 2017.

[23] Xiao, Z, Xia, P., and Xia, X *"Channel estimation and hybrid precoding for millimeter-wave MIMO systems: A low complexity overall solution,*" IEEE Access, vol. 5, pp. 16100-16110, 2020. https://doi.org.10.1109/OJCOMS.2020.3015394

[24] Ayach, O., Rajagopal, S., Abu-Surra, S., Pi, Z., Heath, R.W "*Spatially sparse precoding in millimeter MIMO Systems,"* IEEE Transactions on Wireless Communications, vol. 13, no. 3, pp. 1499-1513,2014.https://doi.org.10.1109/TWC.2014.011714.130846